Journal of Materials Chemistry B

ROYAL SOCIETY OF CHEMISTRY

PAPER

View Article Online
View Journal | View Issue

Cite this: J. Mater. Chem. B, 2024, 12, 10409

Potent BODIPY-based photosensitisers for selective mitochondrial dysfunction and effective photodynamic therapy†

Edward R. H. Walter, ‡[ab] Peter Kam-Keung Leung, ‡[cd] Lawrence Cho-Cheung Lee, [bc] Kenneth Kam-Wing Lo *[cd] and Nicholas J. Long *[a]

Received 23rd July 2024,
Accepted 5th September 2024

DOI: 10.1039/d4tb01609b

rsc.li/materials-b

The development of new and improved mitochondria-targeting photosensitisers (PSs) for photodynamic therapy (PDT) remains highly desirable, due to the critical role the mitochondria play in maintaining healthy cellular function. Here, we report the design, synthesis, photophysical properties and biological characterisation of a series of di-iodinated BODIPY-based PSs, **BODIPY-Mito-I-*n***, for mitochondria-targeted PDT applications. Six **BODIPY-Mito-I-*n*** analogues were synthesised in good yields, with fast reaction times of between 30 and 60 min under mild conditions. The di-iodination of the BODIPY scaffold enabled highly efficient population of the triplet state, leading to high singlet oxygen ($^1O_2$) photosensitisation efficiencies (Φ_Δ = 0.55–0.65). All **BODIPY-Mito-I-*n*** compounds exhibited very high photocytotoxic activity towards HeLa cells, with $IC_{50,light}$ values of between 1.30 and 6.93 nM, due to photoinduced $^1O_2$ generation. Notably, the poly(ethylene glycol) (PEG)-modified **BODIPY-Mito-I-6** showed remarkably lower dark cytotoxicity ($IC_{50,dark}$ = 6.68–7.25 μM) than the non-PEGylated analogues **BODIPY-Mito-I-1** to **BODIPY-Mito-I-5** ($IC_{50,dark}$ = 0.58–1.09 μM), resulting in photocytotoxicity indices up to 2120. Mechanistic studies revealed that **BODIPY-Mito-I-6** induced reactive oxygen species overproduction and mitochondrial dysfunction in cells upon irradiation, leading to significant cell death through a combination of apoptosis and necrosis. It is anticipated that our design will contribute to the development of more effective mitochondria-targeting PSs for cancer therapy.

Introduction

Mitochondria are small subcellular organelles involved in a wide range of essential biological processes.[1,2] Mitochondria display a negative membrane potential (MMP, $\Delta\psi_m$),[3] as a consequence of a proton gradient across the inner mitochondrial membrane.[4] Therefore, lipophilic cations such as triphenylphosphonium (TPP^+) preferentially accumulate in the mitochondria over other cellular compartments.[5] Additionally, the MMP is known to be significantly elevated in cancer and cardiovascular disease,[6] enabling TPP^+-based compounds to be utilised in mitochondrial imaging[7,8] and therapeutic applications.[9]

Photodynamic therapy (PDT) is a minimally invasive and emerging cancer therapy that has been approved clinically for many different types of cancer.[10] PDT utilises photosensitisers (PSs), compounds that produce reactive oxygen species (ROS) such as singlet oxygen ($^1O_2$) upon irradiation with light.[11] Importantly, targeting PSs to cancer cells results in a highly localised treatment, minimising the side effects for the patient.

Over the last decade a wide range of mitochondria-targeting PSs have been reported, including boron-dipyrromethenes (BODIPYs),[12,13] cyanines,[14] hemicyanines,[15] porphyrins,[16] cyclometallated iridium(III) complexes,[17,18] and a promising iridium(III)–BODIPY conjugate for triple-negative breast cancer cells.[19] Such an approach is a highly effective cancer therapy, due to the important role of the mitochondria in energy production and modulating cellular function.

Halogenated BODIPYs are widely used as PSs due to their high photostability, tuneable absorption wavelengths and efficient population of the triplet excited states *via* intersystem

[a] Department of Chemistry, Imperial College London, Molecular Sciences Research Hub, London, W12 0BZ, UK. E-mail: n.long@imperial.ac.uk
[b] Laboratory for Synthetic Chemistry and Chemical Biology Limited, Units 1503-1511, 15/F, Building 17 W, Hong Kong Science Park, New Territories, Hong Kong, P. R. China
[c] Department of Chemistry, City University of Hong Kong, Tat Chee Avenue, Kowloon, Hong Kong, P. R. China. E-mail: bhkenlo@cityu.edu.hk
[d] State Key Laboratory of Terahertz and Millimetre Waves, City University of Hong Kong, Tat Chee Avenue, Kowloon, Hong Kong, P. R. China

† Electronic supplementary information (ESI) available: Details of synthesis, and photophysical and biological characterisation of all compounds used in the study. See DOI: https://doi.org/10.1039/d4tb01609b

‡ Equal contribution from both authors.

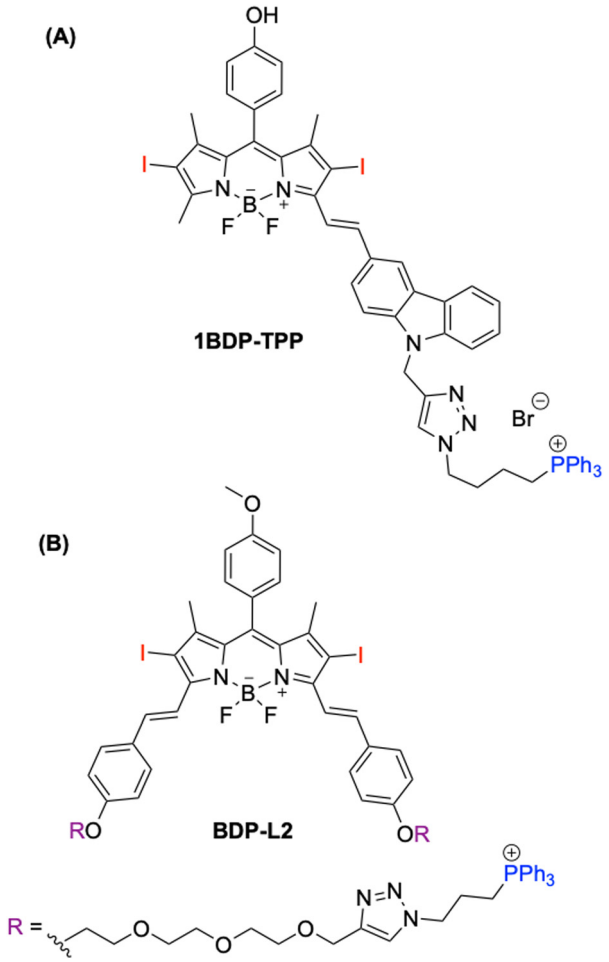

Fig. 1 Literature examples of TPP^+-based BODIPY PSs. (A) **1BDP-TPP** developed by Guo and co-workers[29] and (B) **BDP-L2** developed by Huang and co-workers.[30]

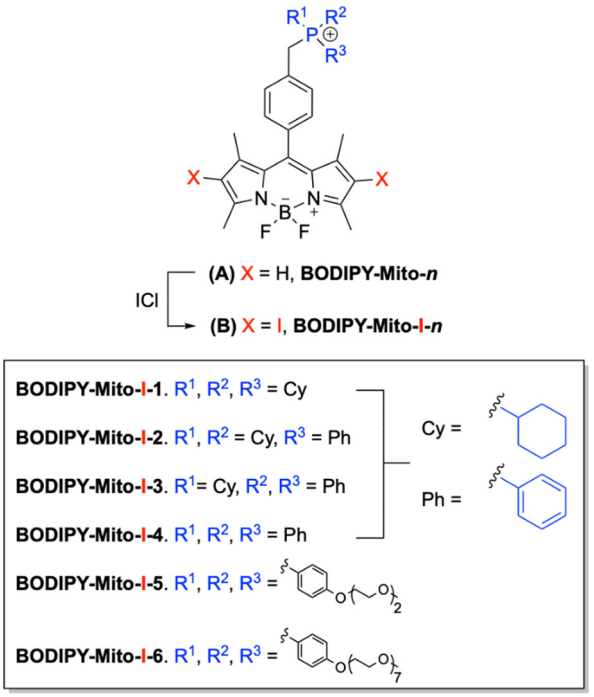

Fig. 2 (A) Structures of fluorescent **BODIPY-Mito-*n***[32] and (B) their di-iodinated counterparts, **BODIPY-Mito-I-*n***, described in this study.

crossing (ISC).[20–22] Furthermore, the BODIPY structure can be easily modified to fine-tune photophysical properties and facilitate the introduction of functional handles, such as targeting units,[7,8] water-solubilising groups,[23] and other therapeutic modalities for synergistic therapy approaches.[24–26]

The utilisation of halogenated BODIPYs with a TPP^+ moiety for developing mitochondria-targeting PSs in PDT applications remains relatively unexplored.[27–31] Examples in the literature show promise; for example, **1BDP-TPP** developed by Guo and co-workers displaying an encouraging photocytotoxicity index (PI; $IC_{50,dark}/IC_{50light}$) of 720 in MCF-7 cells (Fig. 1A).[29] Additionally, Huang and co-workers improved the solubility of **BDP-L2** solubility through the addition of a triethylene glycol linker (Fig. 1B).[30]

However, no detailed studies have been carried out to fine tune these photophysical characteristics by varying the alkyl/aryl moiety on the phosphonium cation, in an attempt to further enhance the PI values. As such, compounds displaying both a large PI value and excellent water solubility remain highly sought-after. Furthermore, through the modification of substituents on the phosphonium cation, results are directly transferable to facilitate the development of a new generation of mitochondria-targeting compounds for imaging and therapy.

In our previous work we reported a series of biocompatible fluorescent BODIPY-based compounds, **BODIPY-Mito-*n***, bearing cyclohexyl or phenyl functionalities.[32] Additionally, analogues possessing improved water solubility were developed through the incorporation of di(ethylene glycol) (DEG) and poly(ethylene glycol) (PEG) moieties (Fig. 2A). All compounds exhibited high mitochondrial specificity (Pearson's correlation coefficients (PCCs) between 0.76 and 0.96) and excellent MMP-sensitivity. However, PEGylated (n = 7) **BODIPY-Mito-6** was found to have the highest MMP-sensitive localisation, with a 75% decrease in the fluorescence intensity following MMP depolarisation.

We report herein the design, synthesis and characterisation of a series of di-iodinated BODIPY-based PSs, **BODIPY-Mito-I-*n***(Fig. 2B). These PSs were designed based on our previously developed versatile BODIPY scaffolds.[32] However, di-iodination promotes $^1O_2$ production as a result of ISC to the triplet excited states, and enables such probes to be used as mitochondria-targeting PSs instead of fluorescent imaging agents.[20–22] Analogues **BODIPY-Mito-I-1** to **BODIPY-Mito-I-4** vary by the number of cyclohexyl- and phenyl moieties on the phosphonium cation, to gain a deeper understanding on how this modulates their dark cytotoxicity and photocytotoxicity. However, one major limitation of current PSs is poor water solubility due to aggregation in aqueous media.[33] Therefore, analogues incorporating DEG (**BODIPY-Mito-I-5**) and PEG (**BODIPY-Mito-I-6**) functionalities were developed in an attempt to improve water solubility and lower dark cytotoxicity to achieve an enhanced phototherapeutic efficacy.

Results and discussion

Design and synthesis of BODIPY-Mito-I-*n* analogues

Compounds **BODIPY-Mito-I-*n*** were synthesised in a one-step reaction from their **BODIPY-Mito-*n*** precursors, using iodine monochloride under mild conditions and fast reaction times of between 30 and 60 min (Scheme 1). Following purification by silica gel column chromatography, **BODIPY-Mito-I-*n*** analogues were all isolated in good yields of between 60 and 76%. Furthermore, the incorporation of DEG and PEG moieties for **BODIPY-Mito-I-5** and **BODIPY-Mito-I-6**, respectively, significantly enhanced aqueous solubility.

Di-iodination of the β-pyrrolic position of BODIPY (**1**) prior to functionalisation with TPP^+ was also attempted (Scheme 2). However, it was found that alkylation of (**2**), previously synthesised in a procedure from Zhang and co-workers,[35] with triphenylphosphine resulted in the removal of the iodine atoms, and the partial regeneration of the non-iodinated compound (**1**).

Photophysical and photochemical properties of BODIPY-Mito-I-*n* analogues

The photophysical properties of **BODIPY-Mito-I-*n*** analogues were recorded in phosphate-buffered saline (PBS) (pH = 7.4) and acetonitrile (Table 1, Fig. 3 and Fig. S1, S2, ESI†) for comparison with our previously reported **BODIPY-Mito-*n*** series.[32]

In aqueous media, **BODIPY-Mito-I-*n*** compounds showed considerably broader absorption spectra (Fig. 1) when compared to acetonitrile (Fig. S1, ESI†). Additionally, **BODIPY-Mito-I-*n*** compounds displayed low fluorescence quantum yields (Φ_{em} = 0.016–0.020), due to efficient ISC from the singlet (S_1) to triplet (T_1) excited state following di-iodination (Table 1). A weaker emission intensity was displayed in aqueous environments across the series when compared to acetonitrile (Fig. 3B and Fig. S2, ESI†). Therefore, a further reduction in the fluorescence quantum yields was displayed ($\Phi_{em} \leq 0.004$), and is likely attributed to the increased aggregation of **BODIPY-Mito-I-*n*** analogues in aqueous media.

The introduction of DEG (**BODIPY-Mito-I-5**) and PEG (**BODIPY-Mito-I-6**) moieties resulted in a blue shift in the absorption (Fig. 3A) and emission wavelength maximum (Fig. S2, ESI†), as well as a small increase in the fluorescence quantum yield (Table 1). However, due to the similarity of photophysical properties displayed for **BODIPY-Mito-I-*n*** analogues in acetonitrile, it is expected that such characteristics are as a result of reduced aggregation following the installation of hydrophilic DEG or PEG moieties.

Singlet oxygen generation of BODIPY-Mito-I-*n* analogues

The $^1O_2$ quantum yields (Φ_Δ) of **BODIPY-Mito-I-*n*** analogues were determined *via* the indirect method (Table 2), using 1,3-diphenylisobenzofuran (DPBF) as the $^1O_2$ scavenger.[36] Methanol was chosen as a solvent due to enhanced solubility of molecular oxygen.[37] The Φ_Δ values were also recorded in acetonitrile, to compliment the photophysical characterisation of our **BODIPY-Mito-I-*n*** analogues.

Following irradiation at 525 nm for 10 s intervals, a decrease in the DPBF absorbance at 411 nm was observed in both methanol (Fig. S3 and S4, ESI†) and acetonitrile, (Fig. S5 and S6, ESI†), confirming the generation of $^1O_2$. All **BODIPY-Mito-I-*n*** analogues displayed high $^1O_2$ photosensitisation efficiencies between 0.60–0.65 in methanol and 0.55–0.63 in acetonitrile (Table 2), through the promotion of ISC from the S_1 to the T_1

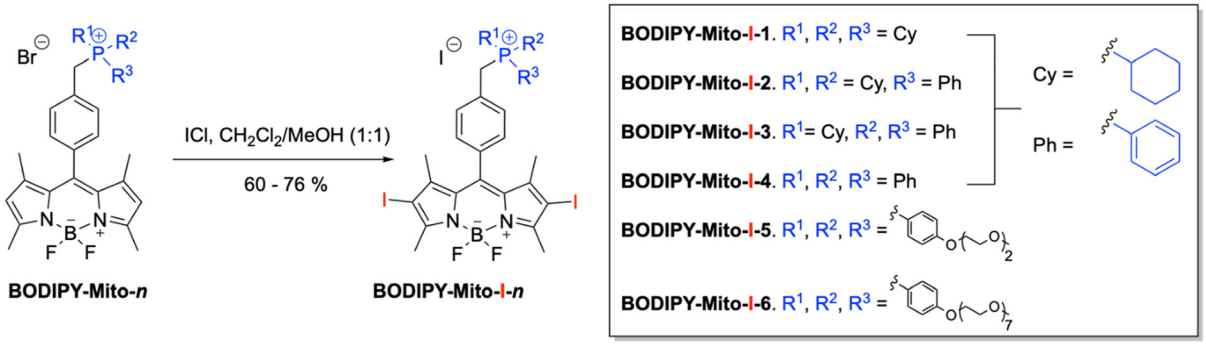

Scheme 1 Synthesis of **BODIPY-Mito-I-*n*** compounds.

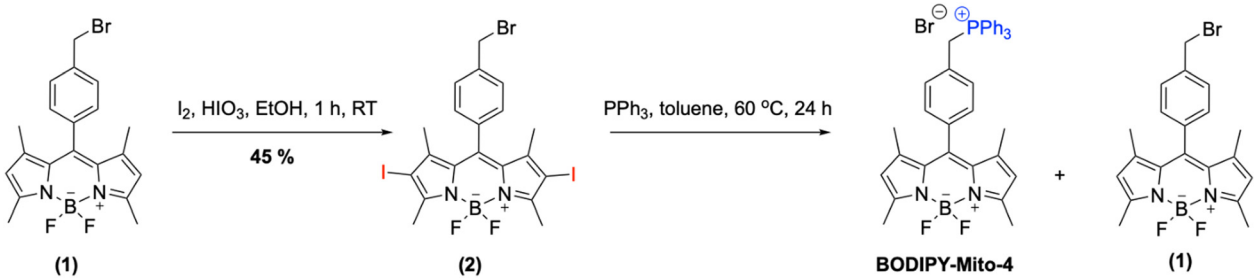

Scheme 2 Attempted synthesis of **BODIPY-Mito-4** from BODIPY (**1**).

Table 1 Photophysical data of **BODIPY-Mito-I-*n*** compounds in PBS (pH = 7.4) and acetonitrile.[a] Compounds **BODIPY-Mito-4** and **BODIPY-Mito-6** from our previous work is added for comparison[32]

Compound	Medium	λ_{abs}/nm (ε/10^4 M^{-1} cm^{-1})	λ_{ex}/nm	λ_{em}/nm	Φ_{em}
This work					
BODIPY-Mito-I-1	PBS	514 (2.10), 542 (2.61)	535	575[b]	<0.001
	CH_3CN	532 (6.81)	534	553	0.018
BODIPY-Mito-I-2	PBS	514 (2.13), 544 (2.50)	535	579[b]	<0.001
	CH_3CN	532 (7.09)	535	553	0.019
BODIPY-Mito-I-3	PBS	514 (2.09), 542 (2.49)	532	576[b]	<0.001
	CH_3CN	532 (7.02)	535	552	0.019
BODIPY-Mito-I-4	PBS	514 (2.28), 545 (2.74)	540	588[b]	<0.001
	CH_3CN	532 (8.18)	535	554	0.017
BODIPY-Mito-I-5	PBS	517 (2.33), 539 (2.54)	534	575[b]	0.002
	CH_3CN	532 (6.85)	535	552	0.020
BODIPY-Mito-I-6	PBS	515 (2.92), 537 (4.06)	534	557[b]	0.004
	CH_3CN	532 (7.39)	536	553	0.016
Previous work[32]					
BODIPY-Mito-4	PBS	497 (5.92)	497	511	0.59
	CH_3CN	499[c]	500	512	0.57
BODIPY-Mito-6	PBS	498 (6.49)	500	512	0.72
	CH_3CN	499[c]	504	513	0.60

[a] [**BODIPY**] = 10 μM, 298 K. Quantum yields (Φ) ± 20% were measured using rhodamine 6G in ethanol (Φ_{488nm} = 0.94)[34] as the standard. [b] Very weak emission was observed. [c] The extinction coefficient (ε) in CH_3CN was not reported.

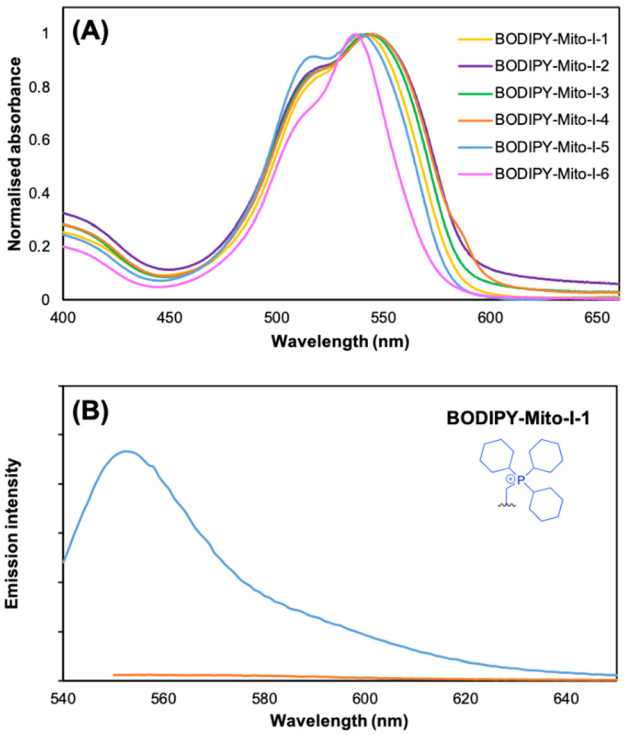

Fig. 3 (A) Absorption spectra of **BODIPY-Mito-I-*n*** analogues in PBS (pH = 7.4). (B) Emission spectra of **BODIPY-Mito-I-1** in CH_3CN (blue, λ_{ex} = 532 nm) and PBS (pH = 7.4) (orange, λ_{ex} = 539 nm). [**BODIPY**] = 10 μM, 298 K.

excited state due to the heavy atom effect. It has previously been reported that Φ_Δ decreases following PEGylation (PEG average M_w = 5000 Da).[36] However, in our case, following the introduction of three PEG moieties with a lower molecular weight (PEG average M_w = 350 Da), no decrease in Φ_Δ was observed.

Furthermore, no significant changes in the absorption at 525 nm were observed for **BODIPY-Mito-I-*n*** analogues under the same irradiation conditions. Additionally, the $^1O_2$ generation efficiency of **BODIPY-Mito-*n*** analogues without di-iodination, was 4.3- and 4.6-fold lower for previously synthesised[32] **BODIPY-Mito-1** (Φ_Δ = 0.15) and **BODIPY-Mito-6** (Φ_Δ = 0.13), respectively, in methanol (Fig. S7, ESI†). Therefore, di-iodination is essential in facilitating efficient $^1O_2$ generation.

Table 2 $^1O_2$ quantum yields (Φ_Δ) of **BODIPY-Mito-I-*n*** compounds in aerated methanol and acetonitrile with DPBF as the $^1O_2$ scavenger[a]

Compound	Medium	Φ_Δ
BODIPY-Mito-I-1	CH_3OH	0.64[b]
	CH_3CN	0.63[c]
BODIPY-Mito-I-2	CH_3OH	0.61[b]
	CH_3CN	0.55[c]
BODIPY-Mito-I-3	CH_3OH	0.60[b]
	CH_3CN	0.56[c]
BODIPY-Mito-I-4	CH_3OH	0.65[b]
	CH_3CN	0.60[c]
BODIPY-Mito-I-5	CH_3OH	0.60[b]
	CH_3CN	0.63[c]
BODIPY-Mito-I-6	CH_3OH	0.61[b]
	CH_3CN	0.62[c]

[a] [**BODIPY**] = 0.5 μM, [DPBF] = 50 μM, 298 K. [b] Φ_Δ were measured using Rose Bengal in aerated methanol (Φ_Δ = 0.79) as the standard.[38] [c] Φ_Δ were measured using Rose Bengal in aerated acetonitrile (Φ_Δ = 0.53) as the standard.[39]

(Photo)cytotoxicity of BODIPY-Mito-I-*n* analogues

The (photo)cytotoxicity of **BODIPY-Mito-I-*n*** analogues towards HeLa cells was examined using the 3-(4,5-dimethylthiazol-2-yl)-2,5-diphenyltetrazolium bromide (MTT) and neutral red uptake (NRU) assays. The MTT assay measures cellular metabolic activity as an indicator of cell viability, while the NRU assay measures the ability of viable cells to incorporate and bind neutral red in lysosomes. The use of two different cell viability assays can help avoid possible artefacts caused by the mitochondrial localisation of the PSs, which might disrupt mitochondrial activity and cellular metabolism.

Table 3 (Photo)cytotoxicity (IC_{50}) of the **BODIPY-Mito-I-*n*** compounds towards HeLa cells determined by the MTT and NRU assays. The cells were first incubated with the **BODIPY-Mito-I-*n*** compounds in the dark for 24 h, then washed thoroughly with PBS, incubated in the dark or irradiated at 525 nm (10 mW cm^{-2}) for 10 min, and subsequently incubated in the dark for 20 h. PI = $IC_{50,dark}/IC_{50,light}$

	MTT			NRU		
Compound	$IC_{50,dark}$/μM	$IC_{50,light}$/nM	PI	$IC_{50,dark}$/μM	$IC_{50,light}$/nM	PI
BODIPY-Mito-I-1	0.81 ± 0.018	1.72 ± 0.055	471	0.72 ± 0.022	1.71 ± 0.060	421
BODIPY-Mito-I-2	0.59 ± 0.074	1.30 ± 0.050	454	0.58 ± 0.072	1.41 ± 0.095	411
BODIPY-Mito-I-3	0.78 ± 0.040	1.46 ± 0.093	534	0.73 ± 0.071	1.66 ± 0.113	440
BODIPY-Mito-I-4	0.66 ± 0.045	1.53 ± 0.064	431	0.62 ± 0.059	1.60 ± 0.073	388
BODIPY-Mito-I-5	1.02 ± 0.093	6.93 ± 0.487	147	1.09 ± 0.083	6.63 ± 0.562	164
BODIPY-Mito-I-6	7.25 ± 0.571	4.22 ± 1.090	1718	6.68 ± 1.009	3.15 ± 0.141	2120

Upon incubation in the dark for 24 h, the **BODIPY-Mito-I-*n*** analogues displayed moderate cytotoxic activity towards HeLa cells (Table 3 and Fig. S8, S9, ESI†). The results obtained from the MTT and NRU assays were very similar, revealing $IC_{50,dark}$ values ranging from 0.59 to 7.25 μM and 0.58 to 6.68 μM, respectively (Table 3). Notably, the $IC_{50,dark}$ values of **BODIPY-Mito-I-5** (1.02–1.09 μM) and **BODIPY-Mito-I-6** (6.68–7.25 μM) were higher than those of analogues **BODIPY-Mito-I-1** to **BODIPY-Mito-I-4** (0.58–0.81 μM). The lower dark cytotoxicity of **BODIPY-Mito-I-5** and **BODIPY-Mito-I-6** is attributed to the DEG and PEG pendants on the TPP^+ moiety, respectively, which can reduce non-specific interactions of the compounds with mitochondrial proteins and membrane structures, enhancing their biocompatibility. The lower cellular uptake of these compounds should also be accounted for their reduced dark cytotoxic activity (Fig. S10, ESI†). Previous studies by us[32,40–43] and others[44–46] have also demonstrated that PEGylation could lower the cellular uptake efficiencies of the compounds due to reduced lipophilicity.

Upon irradiation of the treated cells at 525 nm (10 mW cm^{-2}) for 10 min, the cytotoxic activity of the **BODIPY-Mito-I-*n*** analogues was significantly enhanced ($IC_{50,light}$ = 1.30–6.93 nM), resulting in PI values of 147 to 2120 (Table 3). The high photocytotoxicity of the compounds is ascribed to their high $^1O_2$ generation efficiencies (Φ_Δ = 0.60–0.65 in methanol; Table 2). Among these compounds, **BODIPY-Mito-I-6** exhibited the largest PI value (2120) due to its low dark cytotoxicity ($IC_{50,dark}$ = 6.68–7.25 μM) and high photocytotoxicity ($IC_{50,light}$ = 3.15–4.22 nM). To the best of our knowledge, PI values of 1718 and 2120 in HeLa cells for **BODIPY-Mito-I-6**, determined by the MTT and NRU assay, respectively, are the highest reported for a TPP^+-functionalised BODIPY-based compound.[22,29–31] Such a result highlights the importance of using multiple PEG moieties to enhance the phototherapeutic efficacy of BODIPY-based PSs in cells.[12,13]

Mechanism of cell death induced by BODIPY-Mito-I-*n* analogues

Although the intracellular localisation of the **BODIPY-Mito-I-*n*** compounds could not be accurately determined by confocal microscopy due to their very low fluorescence quantum yields (≤0.004; Table 1), they should presumably exhibit similar localisation properties as their non-iodinated counterparts and localise in the mitochondria because iodination of the BODIPY scaffold should not pose a significant impact on their cellular localisation.[12,27,31] Therefore, it is likely that the effective photoinduced generation of $^1O_2$ by these compounds in the mitochondria induced mitochondrial dysfunction and triggered cell death, leading to the very high photocytotoxicity. To validate that the **BODIPY-Mito-I-*n*** analogues can generate ROS inside cells, we used CM-H_2DCFDA, a cell-permeable, non-fluorescent probe that generates a strongly fluorescent 2′,7′-dichlorofluorescein derivative upon oxidation by ROS, to examine intracellular ROS generation. Treatment of HeLa cells with **BODIPY-Mito-I-6** in the dark resulted in extremely weak fluorescence (Fig. 4, top). However, strong fluorescence was detected upon exposure of the **BODIPY-Mito-I-6**-loaded cells to irradiation, indicating efficient ROS production by **BODIPY-Mito-I-6** inside cells upon irradiation. We also utilised rhodamine 123 (R123), a fluorescent mitochondrial stain that localises in the mitochondria in an MMP-dependant manner, to monitor changes in MMP upon the treatment. The bright green fluorescence and intact

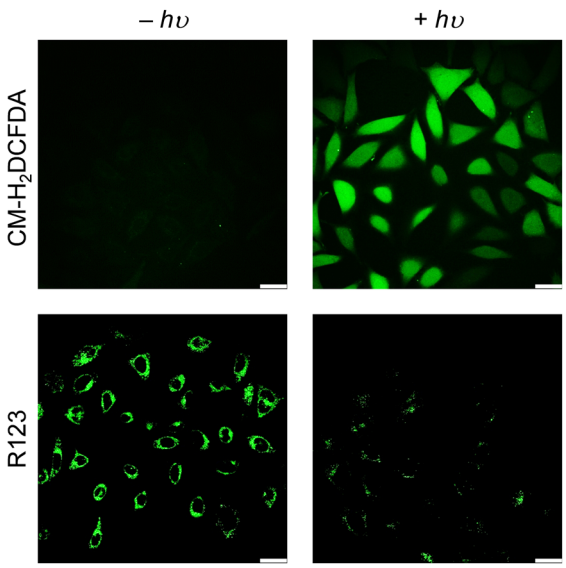

Fig. 4 Analysis of (top) intracellular ROS generation and (bottom) MMP alternation in HeLa cells under different conditions. The cells were first treated with **BODIPY-Mito-I-6** (25 μM, 2 h) and then remained in the dark or irradiated (525 nm, 10 mW cm^{-2}) for 10 min. All the samples were stained with CM-H_2DCFDA (5 μM, 30 min; λ_{ex} = 488 nm, λ_{em} = 500–550 nm) or R123 (5 μM, 15 min; λ_{ex} = 488 nm, λ_{em} = 500–550 nm) prior to microscope imaging. Scale bar = 25 μm.

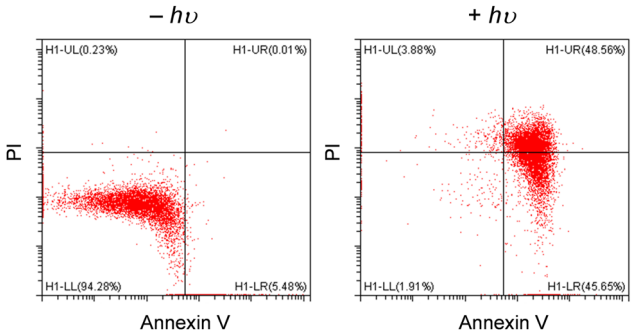

Fig. 5 Flow cytometric analysis of HeLa cells treated with **BODIPY-Mito-I-6** (25 nM, 24 h), remained in the dark or irradiated (525 nm, 10 mW cm^{-2}) for 10 min, and then incubated in fresh medium for 20 h. The cells were then stained with Alexa Fluor 647–Annexin V conjugate and PI and analysed by flow cytometry using 488 and 638 nm excitation.

mitochondrial morphology observed in the cells treated with **BODIPY-Mito-I-6** in the dark (Fig. 4, bottom) indicate that the MMP remained stable. However, upon irradiation, the fluorescence intensity of R123 in **BODIPY-Mito-I-6**-loaded cells decreased substantially, suggesting a significant reduction in MMP. These results collectively illustrate that **BODIPY-Mito-I-6** triggered ROS overproduction and mitochondrial depolarisation in cells upon irradiation, leading to mitochondrial dysfunction and significant cell death. We further studied the mechanism of cell death in **BODIPY-Mito-I-6**-treated cells using the Annexin V/propidium iodide (PI) staining assay. Incubation of the cells with **BODIPY-Mito-I-6** in the dark for 24 h results in a high live cell population (Annexin V^-/PI^-; 94.3%) (Fig. 5). However, upon irradiation, the population of early apoptotic cells (Annexin V^+/PI^-) and late apoptotic/necrotic cells (Annexin V^+/PI^+) significantly increased from 5.48 and 0.01% to 45.65 and 45.86%, respectively, indicating that the cell death pathways mediated by **BODIPY-Mito-I-6** under light conditions involved apoptosis and necrosis. Similar cell death pathways were also observed in cells treated with **BODIPY-Mito-I-1** to **BODIPY-Mito-I-5** followed by light irradiation (Fig. S11, ESI†).

Conclusions

In conclusion, a series of **BODIPY-Mito-I-*n*** analogues were designed, synthesised and characterised as mitochondria-targeting PSs for PDT. All six compounds were synthesised in good yields, under mild conditions, and demonstrated fast reaction times of between 30 and 60 min. Additionally, the incorporation of DEG (**BODIPY-Mito-I-5**) and PEG (**BODIPY-Mito-I-6**) functionalities significantly enhanced water solubility.

The di-iodination of the BODIPY scaffold enabled highly efficient population of the T_1 state, resulting in the high $^1O_2$ photosensitisation efficiencies of the compounds of between 0.60–0.65 and 0.55–0.63 in methanol and acetonitrile, respectively. Furthermore, as expected, **BODIPY-Mito-I-*n*** analogues had significantly lower fluorescence quantum yields in both PBS (pH = 7.4) and acetonitrile, compared to the non-iodinated **BODIPY-Mito-*n*** series.

Notably, **BODIPY-Mito-I-6** showed relatively low dark cytotoxicity due to the PEG pendants on the TPP^+ moiety but displayed very high photocytotoxic activity upon irradiation, due to $^1O_2$ generation, leading to a PI value of up to 2120 in HeLa cells. Further studies revealed that **BODIPY-Mito-I-6** induced ROS overproduction and mitochondrial dysfunction in cells upon irradiation, resulting in significant cell death through a combination of both apoptosis and necrosis.

It is anticipated that the use of aryl-PEGylated phosphine precursors will provide a significant improvement on the widely used TPP^+ moiety for developing new mitochondria-targeting PSs for PDT, due to the notable reduction in dark cytotoxicity without sacrificing the $^1O_2$ photosensitisation efficiency of the PSs and mitochondria-targeting ability of the TPP^+ unit. Therefore, we believe that this work will contribute to the development of more effective PDT strategies, providing valuable insights into the design and optimisation of mitochondria-targeting PSs for enhanced cancer treatment.

Author contributions

E. R. H. W., P. K.-K. L., L. C.-C. L., K. K.-W. L. and N. J. L. designed the project. E. R. H. W carried out the synthesis, characterisation, UV-Vis, fluorescence spectroscopy and $^1O_2$ quantum yield measurements of all the compounds. P. K.-K. L. and L. C-.C. L. carried out the biological characterisation and (photo)-cytotoxicity studies. E. R. H. W., P. K.-K. L., L. C.-C. L., K. K.-W. L. and N. J. L. analysed data. E. R. H. W., P. K.-K. L., L. C.-C. L., K. K.-W. L. and N. J. L. wrote the manuscript.

Data availability

We confirm that all the relevant research data is contained with the manuscript and electronic supporting information. No databases have been used and no references to such databases are contained in the manuscript or ESI.†

Conflicts of interest

There are no conflicts to declare.

Acknowledgements

We thank the Laboratory for Synthetic Chemistry and Chemical Biology (LSCCB) under the Health@InnoHK Programme launched by Innovation and Technology Commission, The Government of Hong Kong SAR, P. R. China. The authors also thank Professor Matthew J. Fuchter and his research group at Imperial College London, UK, for use of their 525 nm LED for the determination of $^1O_2$ quantum yields.

References

1 L. D. Zorova, V. A. Popkov, E. Y. Plotnikov, D. N. Silachev, I. B. Pevzner, S. S. Jankauskas, V. A. Babenko, S. D. Zorov,

A. V. Balakireva, M. Juhaszova, S. J. Sollott and D. B. Zorov, *Anal. Biochem.*, 2018, **552**, 50–59.
2 N. Sun, R. J. Youle and T. Finkel, *Mol. Cell*, 2016, **61**, 654–666.
3 M. P. Murphy, *Biochim. Biophys. Acta, Bioenerg.*, 2008, **1777**, 1028–1031.
4 J. Zielonka, J. Joseph, A. Sikora, M. Hardy, O. Ouari, J. Vasquez-Vivar, G. Cheng, M. Lopez and B. Kalyanaraman, *Chem. Rev.*, 2017, **117**, 10043–10120.
5 M. P. Murphy, *Trends Biotechnol.*, 1997, **15**, 326–330.
6 H. M. Begum and K. Shen, *WIREs Mech. Dis.*, 2023, **15**, e1595.
7 B. E. Osborne, T. T. C. Yue, E. C. T. Waters, F. Baark, R. Southworth and N. J. Long, *Dalton Trans.*, 2021, **50**, 14695–14705.
8 S. P. McCluskey, A. Haslop, C. Coello, R. N. Gunn, E. W. Tate, R. Southworth, C. Plisson, N. J. Long and L. A. Wells, *J. Nucl. Med.*, 2019, **60**, 1750–1756.
9 M. P. Murphy and R. C. Hartley, *Nat. Rev. Drug Discovery*, 2018, **17**, 865–886.
10 J. Usuda, H. Kato, T. Okunaka, K. Furukawa, H. Tsutsui, K. Yamada, Y. Suga, H. Honda, Y. Nagatsuka, T. Ohira, M. Tsuboi and T. Hirano, *J. Thorac. Oncol.*, 2006, **1**, 489–493.
11 J. Karges, *Angew. Chem., Int. Ed.*, 2022, **61**, e202112236.
12 I. W. Badon, C. Kim, J. M. Lim, D. K. Mai, T. P. Vales, D. Kang, S. Cho, J. Lee, H.-J. Kim and J. Yang, *J. Mater. Chem. B*, 2022, **10**, 1196–1209.
13 Q. Guan, L.-L. Zhou, Y.-A. Li and Y.-B. Dong, *Inorg. Chem.*, 2018, **57**, 10137–10145.
14 A. P. Thomas, L. Palanikumar, M. T. Jeena, K. Kim and J.-H. Ryu, *Chem. Sci.*, 2017, **8**, 8351–8356.
15 Z. Cheng, S. Benson, L. Mendive-Tapia, E. Nestoros, C. Lochenie, D. Seah, K. Y. Chang, Y. Feng and M. Vendrell, *Angew. Chem., Int. Ed.*, 2024, **63**, e202404587.
16 Satrialdi, Y. Takano, E. Hirata, N. Ushijima, H. Harashima and Y. Yamada, *Nanoscale Adv.*, 2021, **3**, 5919–5927.
17 J.-H. Zhu, G.-X. Xu, J. Shum, L. C.-C. Lee and K. K.-W. Lo, *Chem. Commun.*, 2021, **57**, 12008–12011.
18 L. Huang, P. K.-K. Leung, L. C.-C. Lee, G.-X. Xu, Y.-W. Lam and K. K.-W. Lo, *Chem. Commun.*, 2022, **58**, 10162–10165.
19 L. Qiao, J. Liu, S. Kuang, X. Liao, J. Kou, L. Ji and H. Chao, *Dalton Trans.*, 2021, **50**, 14332–14341.
20 T. Yogo, Y. Urano, Y. Ishitsuka, F. Maniwa and T. Nagano, *J. Am. Chem. Soc.*, 2005, **127**, 12162–12163.
21 E. Bassan, A. Gualandi, P. G. Cozzi and P. Ceroni, *Chem. Sci.*, 2021, **12**, 6607–6628.
22 S. Wang, L. Gai, Y. Chen, X. Ji, H. Lu and Z. Guo, *Chem. Soc. Rev.*, 2024, **53**, 3976–4019.
23 B. Sui, S. Tang, A. W. Woodward, B. Kim and K. D. Belfield, *Eur. J. Org. Chem.*, 2016, **2016**, 2851–2857.
24 A. Kumar, A. Dixit, S. Banerjee, A. Bhattacharyya, A. Garai, A. A. Karande and A. R. Chakravarty, *Med. Chem. Commun.*, 2016, **7**, 1398–1404.
25 K. Mitra, S. Gautam, P. Kondaiah and A. R. Chakravarty, *ChemMedChem*, 2016, **11**, 1956–1967.
26 U. Bhattacharyya, B. Kumar, A. Garai, A. Bhattacharyya, A. Kumar, S. Banerjee, P. Kondaiah and A. R. Chakravarty, *Inorg. Chem.*, 2017, **56**, 12457–12468.
27 Q. Wang, D. K. P. Ng and P.-C. Lo, *J. Mater. Chem. B*, 2018, **6**, 3285–3296.
28 D. Chen, J. Zhang, Y. Tang, X. Huang, J. Shao, W. Si, J. Ji, Q. Zhang, W. Huang and X. Dong, *J. Mater. Chem. B*, 2018, **6**, 4522–4530.
29 M. A. Masood, Y. Wu, Y. Chen, H. Yuan, N. Sher, F. Faiz, S. Yao, F. Qi, M. I. Khan, M. Ahmed, N. Mushtaq, W. He and Z. Guo, *Dyes Pigm.*, 2022, **202**, 110255.
30 P. Hu, X.-L. Weng, C.-H. Zhu, D.-C. Yang, J.-Y. Liu, Z. Chen and M. Huang, *ChemPlusChem*, 2022, **87**, e202200158.
31 T. P. Vales, S. Cho, J. Lee, H. T. Bui, D. K. Mai, I. W. Badon, H. Lim, W. Jeong, J.-L. Kim, H.-K. Kim and H.-J. Kim, *J. Mol. Struct.*, 2021, **1246**, 131284.
32 E. R. H. Walter, L. C.-C. Lee, P. K.-K. Leung, K. K.-W. Lo and N. J. Long, *Chem. Sci.*, 2024, **15**, 4846–4852.
33 J. Wu, J. Tian, L. Rui and W. Zhang, *Chem. Commun.*, 2018, **54**, 7629–7632.
34 M. Fischer and J. Georges, *Chem. Phys. Lett.*, 1996, **260**, 115–118.
35 B. Yuan, H. Wu, H. Wang, B. Tang, J. F. Xu and X. Zhang, *Angew. Chem., Int. Ed.*, 2021, **60**, 706–710.
36 G.-X. Xu, L. C.-C. Lee, P. K.-K. Leung, E. C.-L. Mak, J. Shum, K. Y. Zhang, Q. Zhao and K. K.-W. Lo, *Chem. Sci.*, 2023, **14**, 13508–13517.
37 D. Dvoranová, Z. Barbieriková and V. Brezová, *Molecules*, 2014, **19**, 17279–17304.
38 R. W. Redmond and J. N. Gamlin, *Photochem. Photobiol.*, 1999, **70**, 391–475.
39 N. Epelde-Elezcano, V. Martínez-Martínez, E. Peña-Cabrera, C. F. A. Gómez-Durán, I. L. Arbeloa and S. Lacombe, *RSC Adv.*, 2016, **6**, 41991–41998.
40 S. P.-Y. Li, T. S.-M. Tang, K. S.-M. Yiu and K. K.-W. Lo, *Chem. – Eur. J.*, 2012, **18**, 13342–13354.
41 A. W.-T. Choi, M.-W. Louie, S. P.-Y. Li, H.-W. Liu, B. T.-N. Chan, T. C.-Y. Lam, A. C.-C. Lin, S.-H. Cheng and K. K.-W. Lo, *Inorg. Chem.*, 2012, **51**, 13289–13302.
42 S. P.-Y. Li, C. T.-S. Lau, M.-W. Louie, Y.-W. Lam, S. H. Cheng and K. K.-W. Lo, *Biomaterials*, 2013, **34**, 7519–7532.
43 K. K.-S. Tso, K.-K. Leung, H.-W. Liu and K. K.-W. Lo, *Chem. Commun.*, 2016, **52**, 4557–4560.
44 J. Xie, C. Xu, N. Kohler, Y. Hou and S. Sun, *Adv. Mater.*, 2007, **19**, 3163–3166.
45 Y. Guo, H. Yuan, W. L. Rice, A. T. N. Kumar, C. J. Goergen, K. Jokivarsi and L. Josephson, *J. Am. Chem. Soc.*, 2012, **134**, 19338–19341.
46 L. Sanchez, Y. Yi and Y. Yu, *Nanoscale*, 2017, **9**, 288–297.